Redox nanoparticle therapeutics to cancer increase in therapeutic effect of doxorubicin, suppressing its adverse effect

doi: 10.1016/j.jconrel.2013.08.011

Article

Title: Redox Nanoparticle Therapeutics to Cancer –Increase in therapeutic effect of doxorubicin, suppressing its adverse effect–

Authors: Toru Yoshitomi[a], Yuki Ozaki[a], Sindhu Thangavel[a], Yukio Nagasaki[1-3]*

Affiliation:
[a] Department of Materials Sciences, Graduate School of Pure and Applied Sciences, University of Tsukuba, Tennoudai 1-1-1, Tsukuba, Ibaraki, 305-8573, Japan
[b] Master's School of Medical Sciences, Graduate School of Comprehensive Human Sciences, University of Tsukuba, Tennoudai 1-1-1, Tsukuba, Ibaraki, 305-8573, Japan
[c] Satellite Laboratory, International Center for Materials Nanoarchitectonics (WPI-MANA), National Institute for Materials Science (NIMS), University of Tsukuba, Tennoudai 1-1-1, Tsukuba, Ibaraki, 305-8573, Japan

***Corresponding Author:** Yukio Nagasaki, Department of Materials Sciences, Graduate School of Pure and Applied Sciences; Master's School of Medical Sciences, Graduate School of Comprehensive Human Sciences; Satellite Laboratory, International Center for Materials Nanoarchitectonics (WPI-MANA), National Institute for Materials Science (NIMS); University of Tsukuba, Tennoudai 1-1-1, Tsukuba, Ibaraki, 305-8573, Japan
Phone: +81-29-853-5749
Fax: +81-29-853-5749
E-mail information: yukio@nagalabo.jp

Competing Financial Interests statement
No potential conflicts of interest were disclosed.

ABSTRACT

The ultimate goal of chemotherapy is to achieve a cure without causing any adverse effects. We have developed pH-sensitive redox nanoparticle (RNP^N), which disintegrates under acidic conditions and exposes nitroxide radicals, leading to strongly scavenging reactive oxygen species (ROS). After intravenous administration of RNP^N to tumor bearing mice, it effectively accumulated in tumor due to the leaky neovascular and immature lymphatic system and scavenged ROS, resulting in suppression of inflammation and activation of NF-κB, after disintegration of RNP^N in tumor. Pre-administration of RNP^N prior to treatments with anticancer agents, doxorubicin, to tumor-bearing mice significantly suppressed a progression of tumor size, compared to low-molecular weight 4-hydroxy-TEMPO. Interestingly, the administration of RNP^N suppressed adverse effects of doxorubicin to normal organs due to the scavenging ROS and suppression of inflammation, which was confirmed by reduction in lactate dehydrogenase and creatine phosphokinase activities in plasma. RNP^N is thus anticipated as novel and ideal adjuvant for cancer chemotherapy.

Keywords:

Nitroxide radical, pH-responsive polymeric micelle, reactive oxygen species, cancer chemotherapy, doxorubicin, transcriptional factor

Introduction

Despite years of anticancer drug development, including that of molecularly targeted therapeutics with their ability to selectively interfere with certain hallmarks of cancer, no perfect anticancer drug has been developed thus far. Cancer cells are known to develop drug resistance with repeated drug administrations. Recently, chronic inflammation of the tumor microenvironment has been reported to influence such drug resistance [1, 2] . Reactive oxygen species (ROS) generated in this region play an important role [3]. Elevated rates of ROS have been detected in almost all cancers [4], in which they activate transcription factors, such as nuclear factor-kappa B (NF-κB). It has been reported that this NF-κB promotes many aspects of tumor development and progression including an anti-apoptosis effect and drug resistance [5-7]. Interestingly, a large number of anticancer drugs such as the anthracyclines (e.g., doxorubicin [DOX] epirubicin, and daunorubicin), alkylating agents, platinum coordination complexes (e.g., cisplatin, carboplatin, and oxaliplatin), epipodophyllotoxins (e.g., etoposide and teniposide), and camptothecins (e.g., topotecan and irinotecan), generate ROS *in vivo*, resulting in severe adverse effects in normal tissues [8, 9]. At the same time, these anticancer drugs increase oxidative stress in tumor microenvironments and further increase drug resistance in this region. The suppression of inflammation in the tumor microenvironment is one of the suitable targets for decreasing drug resistance of tumor [9-13]. Several approaches have been reported thus far, using anti-inflammatory agents and ROS scavengers such as dexamethasone (DEX) [10-12], edaravone [13], and 2,2,6,6-tetramethylpiperidine-*N*-oxyl (TEMPO) [14]; pretreatment with anti-inflammatory agents or ROS scavengers increases the antitumor activity of anticancer drugs. However, *in vivo*, low-molecular-weight (LMW) drug-based approaches have limited potential because they are rapidly excreted by the kidney [15], resulting in a lower concentration of drug in the tumor area and severe adverse effects in normal tissue; for example, TEMPO derivatives cause dramatic decrease in blood pressure after administration [16]. Additionally, a high enough amount of LMW ROS scavengers cannot be used for the suppression of oxidative stress in the tumor microenvironment, because LMW-TEMPO derivatives induce mitochondrial

dysfunction due to inessential redox reactions in the cells [17, 18].

To address these issues, we have focused on redox polymer therapeutics by using a nitroxide radical-containing nanoparticle (RNP). We developed pH-sensitive RNP (RNP^N), which is a core-shell type of self-assembling polymeric micelle that is 40 nm in diameter, prepared using poly(ethylene glycol)-*b*-poly[4-(2,2,6,6-tetramethylpiperidine-*N*-oxyl)aminomethylstyrene] (PEG-*b*-PMNT) diblock copolymer in aqueous media (Figure 1) [19-22]. As the leakage of the drugs from the nanoparticle into the blood stream would decrease its therapeutic efficiency and cause severe adverse effects, TEMPO moieties were covalently conjugated to the hydrophobic segment of the amphiphilic block copolymer (PEG-*b*-PMNT). There are two main concepts regarding RNP^N for delivering the nitroxide radical TEMPO to the tumor site and effectively scavenging ROS. First, RNP^N exhibits long blood circulation time *in vivo* because of the nanometer-sized structure and high biocompatibility of the PEG outer shell of RNP^N, resulting in the accumulation of RNP^N in inflamed sites including the tumor area, because of the leaky neovascular vessels in this area. Second, RNP^N disintegrates in response to acidic conditions owing to the protonation of amino groups in the PMNT segments. Because of hypoxic effect in tumor microenvironment, extracellular region of tumor is also acidic due to the increased glycolytic system, referred to as Warburg effect [23]. Consequently, RNP^N must disintegrate not only in endosome and lysosome but also in extracellular region of tumor, resulting in increased ROS scavenging activity. Moreover, the adverse effect of LMW nitroxide radicals is markedly suppressed as a result of the compartmentalization of nitroxide radicals in the core of RNP^N in the bloodstream. Given these characteristics, it has so far been confirmed that RNP^N shows not only a suppressive effect on oxidative stress in cellular studies [24, 25] but also a therapeutic effect against ischemia reperfusion injury and intracerebral hemorrhage through intravenous administration *in vivo* [26-28]. If RNP^N accumulates in tumor sites and scavenges ROS effectively, drug resistance of tumor can be successfully prevented by the suppression of NF-κB activation. Another issue in the field of cancer chemotherapy is that the adverse effects of anticancer drugs continue to trouble patients; for example, DOX causes severe cardiovascular toxicity during chemotherapy. As stated previously, since RNP^N tends to improve blood circulation, which increases accumulation in inflamed sites and effectively suppresses inflammation by scavenging the generated ROS in these sites, adverse effects may decrease because of the suppression of ROS caused by DOX in normal tissues. In this study, we investigated the treatment effects of RNP^N on both the anti-tumor activity of DOX and DOX-induced cardiotoxicity *in vivo*.

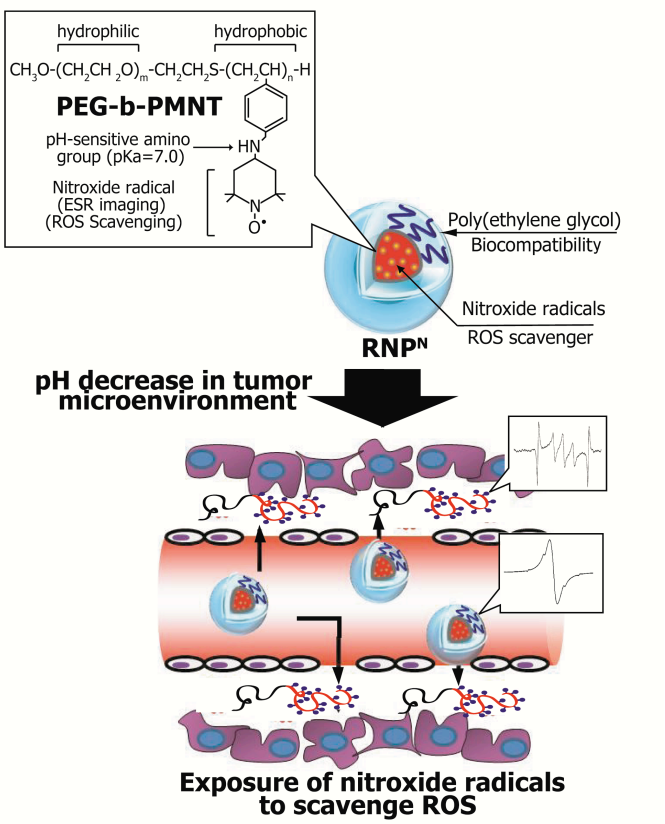

Figure 1. Schematic illustration of (a) pH-sensitive RNP^N, which is a core-shell type of self-assembling polymeric micelle that is 40 nm in diameter and prepared using poly(ethylene glycol)-*b*-poly[4-(2,2,6,6-tetramethylpiperidine-*N*-oxyl)aminomethylstyrene] (PEG-*b*-PMNT) amphiphilic diblock copolymers; and (b) the effective accumulation and disintegration of RNP^N in the tumor area

Material and Methods

Preparation of RNP^N

pH-responsive RNP^N was prepared using self-assembling PEG-*b*-PMNT block copolymers, as previously reported [20]. Please see Supplementary Methods about detailed description of the method.

Animal

The experiments on the enhancement of anticancer activity and cardiotoxicity of DOX were carried out using BALB/c (4 weeks old, male, approximately 25 g) and ICR mice (7 weeks old, male, approximately 35 g), respectively, that were purchased from CHARLES RIVER JAPAN, Inc. Mice were maintained in the experimental animal facilities at the University of Tsukuba. All mice were housed in a temperature- and humidity-controlled, 12-h light:12-h dark environment. All mice were fed commercial chow and water ad libitum. All experiments were performed according to the Guide for the Care and Use of Laboratory Animals of the University of Tsukuba.

Electron spin resonance (ESR) measurement of nitroxide radical concentration in blood and tumors.

The biodistribution of the nitroxide radicals in the RNP^N in tumor-bearing mice was evaluated using ESR. The tumor-bearing mice were prepared with a subcutaneous injection of murine colon adenocarcinoma 26 (colon-26) cells (1×10^6 cells/mouse) into their right thigh. When the volume of the tumor reached 100 mm^3, RNP^N (300 mg/kg) or 4-hydroxy-TEMPO (TEMPOL) (40 mg/kg) was administered to the tumor-bearing mice by intravenous injection. It should be noted that the concentrations of nitroxide radicals in all drugs were the same, which were adjusted using ESR measurements. Blood samples were collected from the heart using a heparinized syringe at 0.083, 0.25, 1, 3, 6 and 24 h after administration, and the tumor was excised immediately after blood collection. The blood and tumor were immediately placed on ice. Plasma samples were then obtained by centrifuging (6,200 rpm, 2000 *g,* for 10 min) the blood samples. To determine the ESR intensities at 0 min, 12.5 μL of RNP^N solution (30 mg/mL) was added to the blood (100 μL), followed by centrifugation (6,200 rpm, 2000 *g,* for 10 min) of the blood and the measurement of ESR, assuming that the total blood volume in mice is 80 mL/kg. The tumor tissue homogenates were prepared using an ultra-sonic homogenizer (UH-50; SMT Company, Tokyo, Japan).

Nitroxide radicals are reduced to hydroxylamine, which has no ESR signal, by an in vivo reducing agent such as ascorbic acid. As hydroxylamine also possesses ROS-scavenging capacity, the total drug concentrations (nitroxide radicals + hydroxylamines) in blood and tumor were determined by the addition of potassium ferricyanide ($K_3[Fe(CN)_6]$) (200 mM, 20 μL) to plasma (200 μL) or the tumor homogenate sample (200 mg) to re-oxidize the hydroxylamines to nitroxide radicals. Using an X-band ESR spectrometer (JES-TE25X; JEOL, Tokyo, Japan), the ESR measurements were carried out under the following conditions: frequency, 9.41 GHz; power, 8.00 mW; field, 333.8 ± 5 mT; sweep time, 1.0 min; modulation, 0.1 mT; and time constant, 0.1 s.

***In vivo* antitumor activity studies**

Tumor-bearing mice were randomly divided into various treatment and control groups (5 mice/group). Animals were treated with saline, RNP^N (100 mg/kg) or LMW-TEMPOL (13.3 mg/kg) by intravenous injection once per day for 4 days before chemotherapy (days -4 to -1). DOX was administered intravenously at a single dose of 10 mg/kg on day 0. Antitumor activity was evaluated in terms of tumor volume (V), which was calculated using the following equation:

$$\text{Tumor volume (V)} = 0.52 \times L \times W^2$$

L and W are the long diameter and the short diameter of the tumor, respectively, as measured by a caliper.

Western blot analysis.

The protein levels of nuclear NF-κB (p65) were measured by Western blotting. The colon 26 cell was used for the *in vitro* study, similar to the *in vivo* study using tumor-bearing mice. The protein from control and RNP^N-treated cells was extracted using a nuclear extraction kit (Cayman Chemical Company, Ann Arbor, MI, USA) according the manufacturer's protocol. Protein estimation was carried out using the Thermo Scientific Pierce BCA Protein Assay Kit (Rockford, IL, USA). Approximately 20 μL of protein sample was electrophoresed in a 15% polyacrylamide gel and transferred to a nitrocellulose membrane (Bio-Rad, Richmond, CA, USA) by electroblotting. The membrane was blocked for 1 h with 1% BSA and probed with

the primary and secondary antibodies. Luminata™ Western HRP Substrate (EMD Millipore Corporation, Billerica, MA, USA) was used to develop the membrane and the protein concentrations were estimated. Each blot was stripped and reprobed for β-actin for equal protein loading detection.

Evaluation of the suppressive effect of RNP^N on cardiotoxicity caused by DOX

The ICR mice were randomly divided to receive an intravenous injection of DOX (20 mg/kg) 30 min after the intravenous injection of RNP^N (25 mg/kg), LMW-TEMPOL (4 mg/kg), or phosphate-buffered saline (PBS), followed by 2 intravenous injections of RNP^N (25 mg/kg), LMW-TEMPOL (4 mg/kg), or PBS at 24 and 48 h after DOX administration. At 72 h after DOX administration, the mice were anesthetized and blood samples were collected by intracardiac puncture using a heparinized syringe. Plasma samples were then obtained by centrifugation (6,200 rpm, 2000 *g,* for 10 min) of the blood. Plasma samples were assayed for plasma lactate dehydrogenase (LDH) and plasma creatine phosphokinase (CPK) activities using a Fuji Dri-chem 3500 analyzer (Fuji-Film, Tokyo, Japan). To determine the amounts of lipid peroxidation and supeoxide induced by DOX, heart tissues were excised from mice after the blood samples were collected. Plasma and heart tissue were frozen and stored at -80 °C until the further use.

Measurement of levels of superoxide anion, TNF-α, and malonyldialdehyde (MDA)

Please see Supplementary Methods about detailed description of the method.

Statistical analysis

All values are expressed as mean ± standard error of mean (SEM). Differences between two groups were examined for statistical significance by using the Student's *t* test. Differences between more than three groups were examined for statistical significance by using one-way ANOVA followed by Tukey's test (SPSS software; IBM Corp, Armonk, NY, USA). A P value of <0.05 was considered significant for all of these statistical analyses.

Results

Biodistribution of RNP^N and its morphological change in tumor sites

PEG-*b*-PMNT block copolymers were prepared as previously reported [20]. RNP^N was prepared by self-assembly of the synthesized amphiphilic block copolymer, PEG-b-PMNT, via the dialysis method against water, with an average diameter of about 40 nm (polydispersity factor, $\mu/\Gamma^2 = 0.04$). To examine the biodistribution of RNP^N and LMW-TEMPOL in tumor-bearing mice, we measured the concentration of nitroxide radicals in the blood and tumor area by ESR, because nitroxide radicals are susceptible to ESR. Figure 2a shows the time profile of the drug concentration of RNP^N and LMW-TEMPOL in the blood. Contrary to the rapid clearance of LMW LMW-TEMPOL from the bloodstream, the ESR signals of RNP^N were observed for a relatively long period of time. The AUC value of RNP^N in blood (AUC: 769.49) was much higher than that of LMW-TEMPOL (AUC: 19.2). The rapid clearance of LMW-TEMPOL might be attributed to preferential renal clearance and diffusion across the entire body. Figure 2b shows the accumulation amounts of RNP^N and LMW-TEMPOL in tumors. The accumulation level of RNP^N in the tumor tissues of mice at 24 h after intravenous administration was 3.3% ID/g tumor tissue, whereas that of LMW-TEMPOL at 24 h after injection was only 0.4% ID/g tumor tissue. Although the accumulation tendency of RNP^N was not markedly higher

than that of RNP^O, another nitroxide radical-containing nanoparticles that is not pH-sensitive and has high colloidal dispersion stability (see Figures S1 and S2), the AUC of RNP^N in tumor tissues (AUC: 39.6) was still 6 to 7 fold higher than that of LMW-TEMPOL (AUC: 6.5). This indicated the clear accumulation of nanoparticles in tumors because of the increased vascular permeation and immature lymphatic excretion (the so-called enhanced permeability and retention [EPR] effect [29]). The moderate accumulation tendency of RNP^N is probably due to the pH-disintegration characteristics (see below) of the polyamine segment, which may loosen its coagulation force coagulation force of hydrophobic interaction in the core by increasing its hydrophilicity. The validity of our strategy regarding the covalent conjugation of bioactive species, nitroxide radicals, in this case, was demonstrated. If the physical entrapment of TEMPO molecules in pH-sensitive nanoparticles is used, they must leak easily during circulation due to the loosened core.

The ESR spectra of RNP^N can provide information on morphological changes *in vivo*. The ESR signal of LMW-TEMPO derivatives shows a sharp triplet due to an interaction between the 14-nitrogen nuclei and the unpaired electron in the dilute solution. At 15 min after the intravenous administration of LMW-TEMPOL to mice, clear triplet signals were observed both in blood and in tumors, as shown in Figures 2c and 2d. In contrast, the ESR signal of RNP^N in the blood stream showed a broad spectrum, because of the confinement of the nitroxide radicals in the solid core of RNP^N (Figure 2e). As shown in Figure 2f, the triplet signals were observed in tumor, indicating the disintegration of RNP^N in this area and the exposed nitroxide radicals outside of the particle, which is probably due to the acidic tumor microenvironment. In fact, no changes in ESR signals for both blood and tumor were observed for RNP^O (Figure S3), leading us to strongly anticipate an increase in the reactivity of the nitroxide radicals of RNP^N to ROS in tumors as a result of its disintegration at the tumor sites.

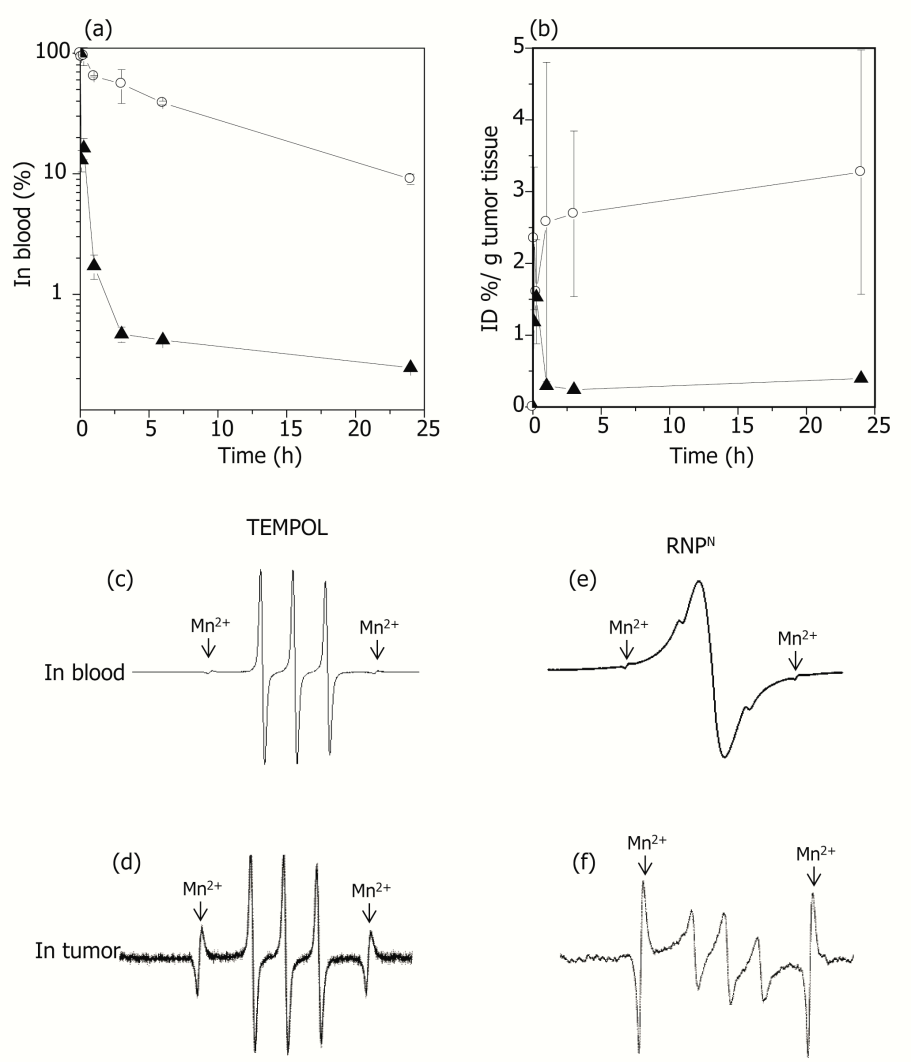

Figure 2. **(a,b)** Distribution profiles of RNP^N (white circle) and low-molecular-weight (LMW) 4-hydroxy-2,2,6,6-tetramethylpiperidine-*N*-oxyl (TEMPOL) (block triangle) in (a) blood and (b) tumor tissue from tumor-bearing mice, as determined by electron spin resonance (ESR) measurement. The data are expressed as means ± SEM; n = 5. **(c-f)** The ESR spectra of (c) LMW-TEMPOL in blood, (d) LMW-TEMPOL in tumor, (e) RNP^N in blood, and (f) RNP^N in tumor at 15 min after intravenous administration are shown. All samples were oxidized by potassium ferricyanide ($K_3[Fe(CN)_6]$).

Pretreatment of tumor-bearing mice with RNP^N enhances the therapeutic effects of DOX *in vivo*

Having confirmed that RNP^N accumulates and disintegrates in tumor regions, we investigated the effect of RNP^N on the expression of NF-κB in cancer cells. Figure 3 shows the expression level of NF-κB in the nuclei of colon-26 cells with and without RNP^N treatment. In contrast to the high expression level of NF-κB observed in the nuclei of tumor cells, the expression level of NF-κB was suppressed, in a dose-dependent manner, on administration of RNP^N, clearly indicating the effectiveness of RNP^N in suppressing this transcription factor in

colon-26 cells.

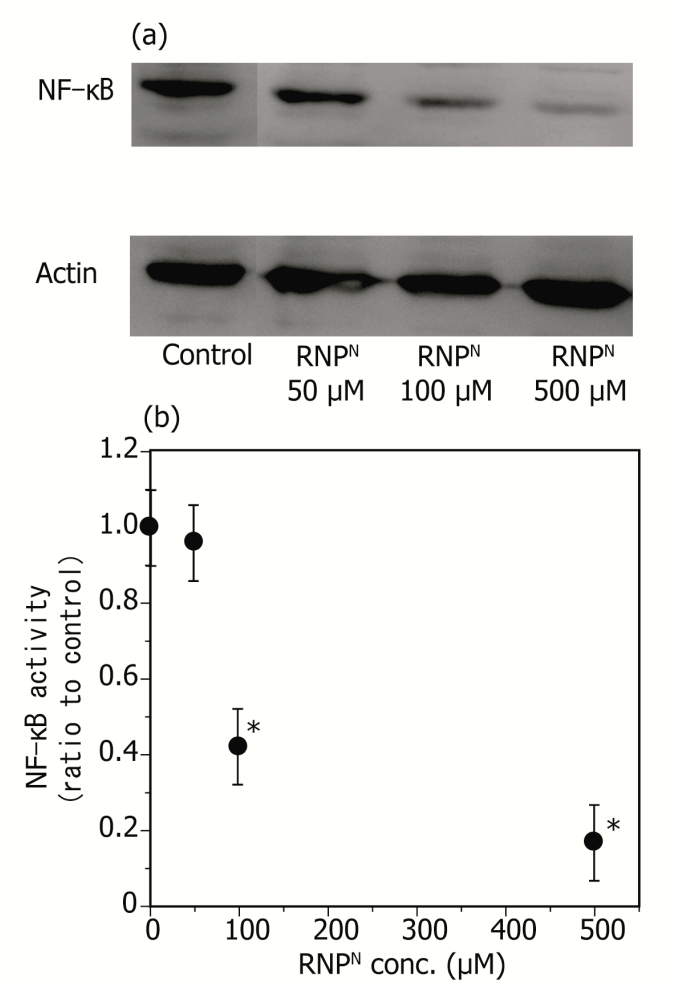

Figure 3. Suppressive effects of RNP^N on the activation of NF-κB. (a) Western blot analysis of NF-κB expression in colon-26 cells treated with RNP^N. (b) The graph represents the densitometry average of three representative blots. Values are expressed as mean ± SEM. **P* < 0.05 compared with controls; Student's *t*-test; n = 3.

Given the significant effect of RNP^N observed on the suppression of inflammatory transcription factor NF-κB, we investigated the pharmacological effect of the anticancer drug, DOX, after pretreatment of tumor-bearing mice with RNP^N. Here, RNP^N was administered for 4 days to suppress the NF-κB activation before DOX treatment. First, we measured the suppressive effect of RNP^N treatment on superoxide generation in the tumor area. Because PEG-b-PMNT possesses nitroxide radicals, it scavenges ROS such as superoxide and hydroxyl radicals [30]. When tumor-bearing mice were treated with intravenous injections of RNP^N at a dose of 100 mg/kg for 4 days, the levels of ROS were found to be significantly decreased in tumors compared with controls (saline administration); this is in sharp contrast to the results observed with administration of LMW-TEMPOL (Figure 4a). The suppression of oxidative stress in the tumor microenvironment was also confirmed by the measurement of the proinflammatory cytokine, TNF-α. As seen in Figure 4b, the suppressive effect of RNP^N treatment on level of

TNF-α was higher than that of LMW-TEMPOL. These findings underline the importance of local ROS scavenging by RNP^N, which results in the suppression of cytokine levels and NF-κB activation [31], resulting in the inhibition of tumor resistance.

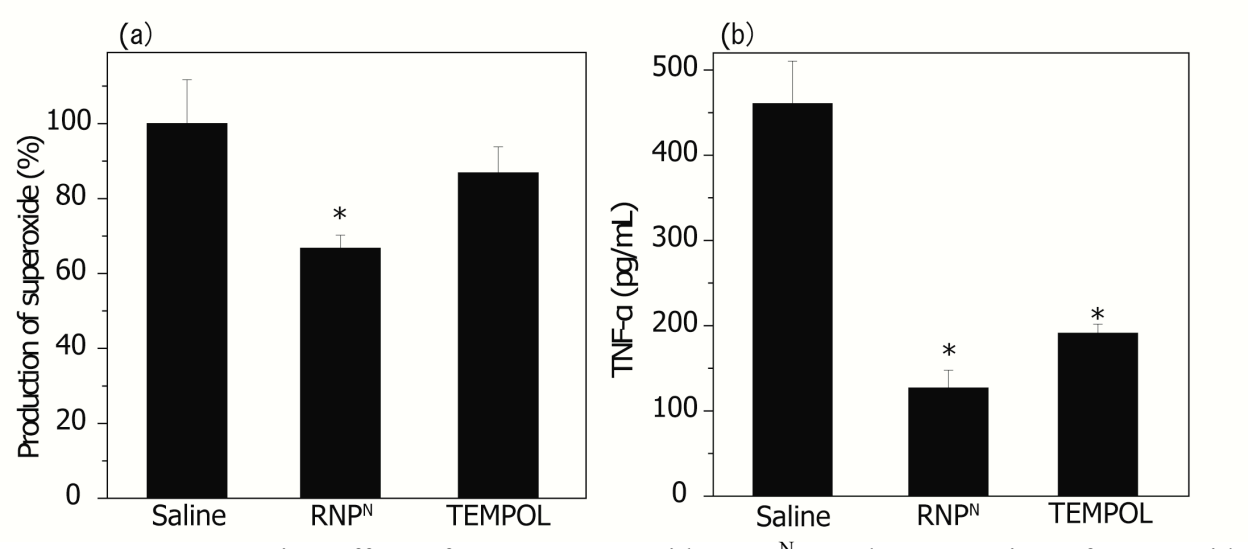

Figure 4. Suppressive effect of pretreatment with RNP^N on the generation of superoxide anions and TNF-α in tumors. (a) Amounts of superoxide in tumor tissue were measured using dihydroethidium (DHE). Superoxide values were expressed as the value related to the fluorescent intensity of the saline group. Values are expressed as mean ± SEM. $*P < 0.05$ compared with the saline group; ANOVA; n = 5. (b) The concentration of TNF-α in tumor was measured by enzyme-linked immunosorbent assay (ELISA). Values are expressed as mean ± SEM. $*P < 0.05$ compared with the saline group; ANOVA; n = 10.

Having demonstrated the suppression of inflammation in the tumor microenvironment and the activation of inflammatory transcription factor NF-κB, we then examined the enhancing effect of RNP^N on the anti-tumor activity of DOX. Tumor-bearing mice were treated with intravenous injections of RNP^N at a dose of 100 mg/kg for 4 days (days -4 to -1), followed by the intravenous injection of DOX (10 mg/kg, day 0). Tumor progression was analyzed as shown in Figure 5. When LMW-TEMPOL was administered intravenously and followed by DOX administration, almost no effect was observed. Although it was previously reported that the intratumoral administration of TEMPO in tumor-bearing mice inhibits tumor growth by inducing apoptosis [14], the intravenous administration of LMW-TEMPOL in tumor-bearing mice did not show any effect under the present study conditions. The reason for these results may stem from a lower intratumoral concentration of nitroxide radicals because of rapid renal clearance and diffusion throughout the entire body. In contrast, a remarkably large effect was observed with the administration of RNP^N prior to DOX administration. Interestingly, a much higher adjuvant effect of RNP^N on the anti-tumor activity of DOX was observed *in vivo* compared with that of RNP^O, although the tumor accumulation of RNP^O was much higher than that of RNP^N (Figure S4). This result indicates that both accumulation tendency and pH-triggered disintegration characteristics of RNP^N are important to effectively suppress the activation of NF-κB and decrease the resistance of tumor cells. Similar effects were observed with the pretreatment of RNP^N prior to the administration of other anticancer drugs, carboplatin (Figure S5).

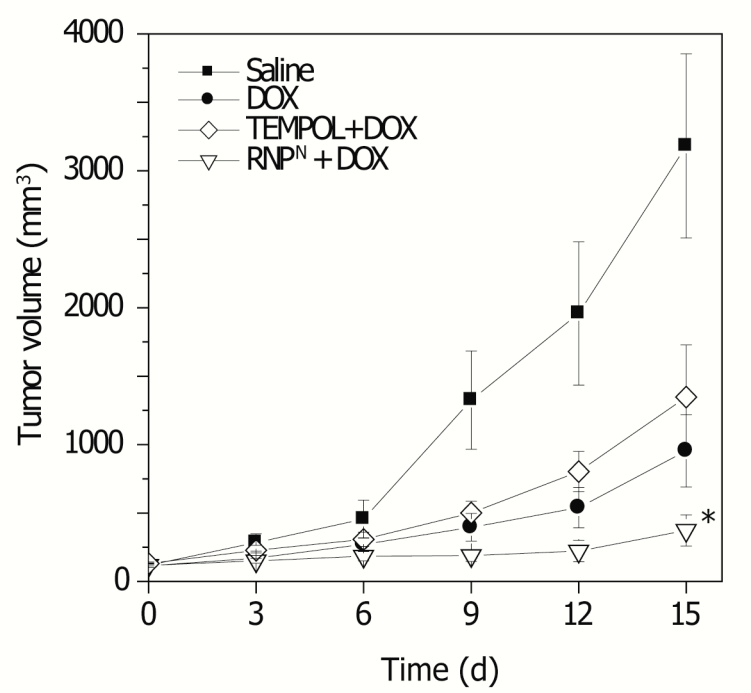

Figure 5. Effect of RNP^N pretreatment on the antitumor activity of doxorubicin (DOX) in BALB/c mice bearing colon-26 tumors. Animals were intravenously pretreated with RNP^N (100 mg/day for 4 days, days -4 to -1). DOX was intravenously administered at a single dose of 10 mg/kg on day 0. Tumor size is expressed as mean ± SEM. $*P < 0.05$ compared with DOX alone; Student's *t*-test; n = 5.

Suppression of adverse effects of DOX by RNP^N

DOX is known to cause cardiotoxicity through the generation of ROS as stated previously. We have already confirmed that RNPs tend to accumulate in inflammation sites and effectively suppress inflammation by scavenging ROS generated in these sites [32]. If RNP^N suppresses the adverse cardiotoxic effects of DOX in addition to inhibiting tumor progression, it would be an ideal cancer chemotherapy system. To examine the cardiotoxicity of DOX, CPK and LDH activities were measured. CPK, LDH, which are indicator of myocardial damage, are released from the heart muscle cells when it is injured. Here, RNP^N or LMW-TEMPOL was administered three times before and after DOX treatment because DOX generates ROS continuously not only in tumor region but also in healthy organs such as heart and liver. As shown in Figures 6a and 6b, compared to that of mice given a tail vein injection of PBS, mice treated with a single dose of DOX (20 mg/kg) showed a 5-fold increase in plasma CPK activity and a 2.9-fold increase in plasma LDH activity. Although the administration of LMW-TEMPOL showed decreases in plasma CPK and LDH activities to some extent in DOX-treated mice, no significant difference was found. In contrast, the administration of RNP^N (100 mg/kg) for 3 days remarkably suppressed cardiotoxicity in DOX-treated mice, as determined by reduction in CPK and LDH. We also investigated whether pretreatment with RNP^N could scavenge ROS, particularly superoxide, generated in the heart at 24 h after DOX administration. As shown in Figure 6c, the generation of ROS in heart tissue was significantly inhibited by RNP^N treatment, regardless of the lack of effect observed with LMW-TEMPOL treatment. Cardiotoxicity was also

investigated by determining the level of lipid peroxidation in the heart after DOX administration. When 20 mg/kg of DOX was administered intravenously, the level of MDA in the heart increased significantly (Figure 6d). In contrast, no increase was observed with a 3-day RNP^N-treatment before and after DOX administration; again, this is in sharp contrast to the findings obtained with LMW-TEMPOL. These results can be attributed to the long circulation time of RNP^N in blood and the accumulation of RNP^N in the inflamed area, followed by the effective scavenging of ROS, resulting in the suppression of cardiotoxicity caused by DOX.

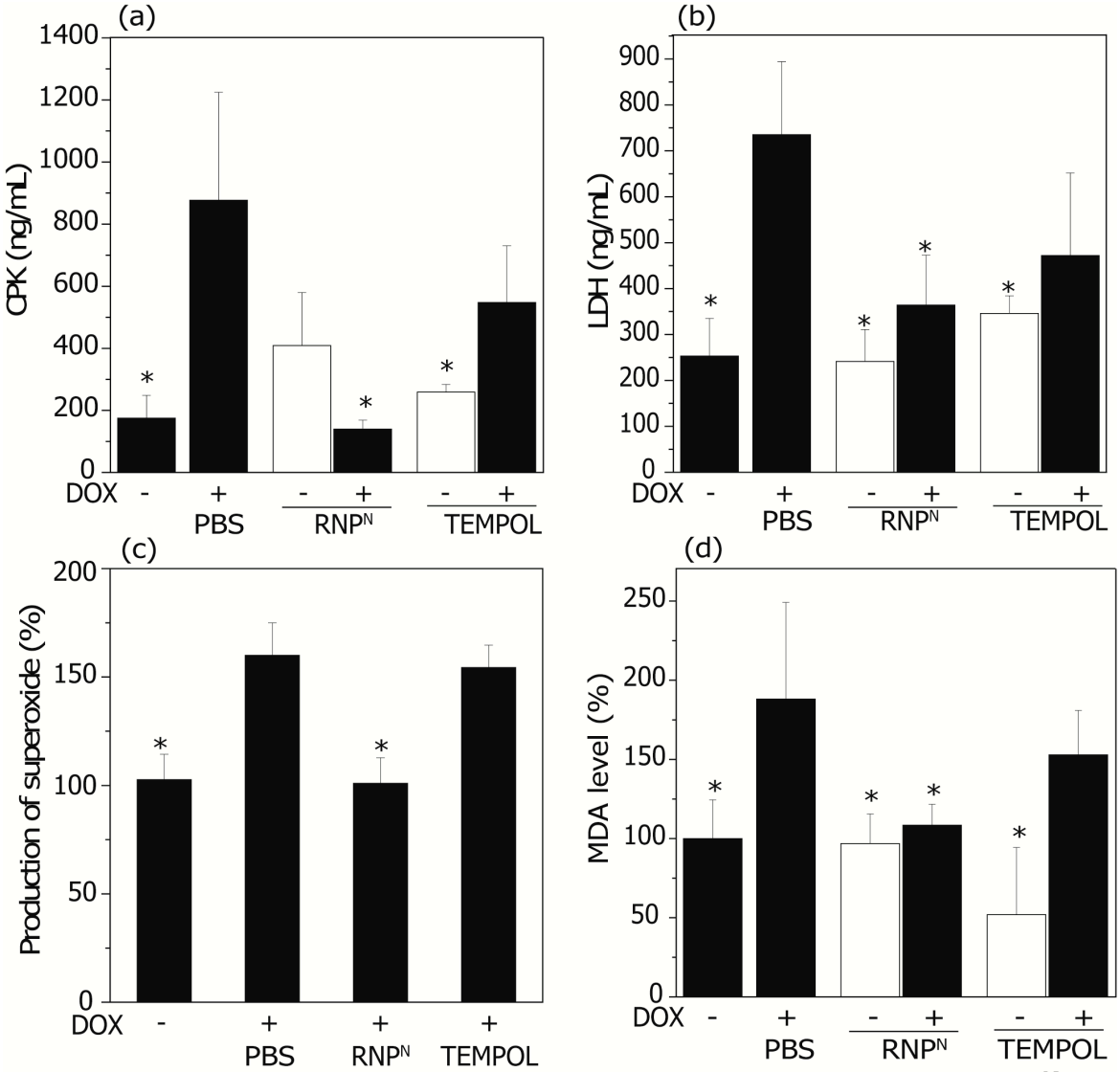

Figure 6. (a,b) Effect of treatment with RNP^N or 4-hydroxy-2,2,6,6-tetramethylpiperidine-*N*-oxyl (TEMPOL) on doxorubicin (DOX)-induced cardiotoxicity, as determined by measurement of the activities of (a) creatine phosphokinase (CPK) and (b) lactate dehydrogenase (LDH) in plasma. The bar graphs represent means ± SEM, $*P < 0.05$ compared with DOX alone; Student's *t*-test; n = 6. (c) Amounts of superoxide in heart tissue were measured using dihydroethidium (DHE). Superoxide values were expressed as the value related to the fluorescent intensity of the control group. Values are expressed as mean ± SEM. $*P < 0.05$ compared with DOX alone; ANOVA; n = 4. (d) Effect of treatment with

RNP^N or LMW-TEMPOL on malonyldialdehyde (MDA) activity in the heart tissue of ICR mice after DOX administration. Values are expressed as mean ± SEM. $*P < 0.05$ compared with DOX alone; Student's *t*-test; n = 6.

Discussion

ROS are involved in the development of a wide spectrum of diseases, including chronic inflammation and cancers. Anticancer drugs administered to cancer patients induce excessive oxidative stress, leading to further inflammation and ROS production. This negative cycle induces the expression of transcription factors such as NF-κB and initiates many factors such as anti-apoptotic effects and drug resistance, leading to tumor development and progression; these factors lower the therapeutic effects of the anticancer drug and cause serious adverse effects. A combination therapy of anticancer drugs with anti-inflammatory agents or ROS scavengers has been developed and applied in treatment. However, this therapy has not been very effective because of the rapid elimination of LMW drugs from the body via renal clearance [15] and the severe adverse effects of the drugs in normal tissues [16-18].

In this study, we demonstrated that RNP^N suppresses the activation of transcription factor, NF-κB in the cancer cells and improves the anticancer effect of DOX in vivo. These results indicate that long-term and effective ROS scavenging at the tumor site by RNP^N pretreatment enhances the anticancer effect of the drug, because of effective accumulation and disintegration of RNP^N in the tumor area. Inflammatory cytokines are also suppressed by RNP^N treatment. Production of ROS and inflammatory cytokines has been proven to be strongly associated with each other [33]. We have observed that ROS scavenging suppresses the production of inflammatory cytokines. RNP^N showed an extended period of circulation in the blood and accumulation in inflamed areas, and the cardiac toxicity of DOX was reduced by RNP^N treatment. Moreover, the anticancer activity and suppression of adverse effects was more remarkably enhanced by RNP^N than by LMW-TEMPOL. Since almost all the anticancer drugs have some drawbacks such as low efficiency and adverse effects, we believe that RNP^N system can help design improved cancer treatments with good therapeutic outcomes, suppressing the adverse effects of the drugs.

Conclusions

In conclusion, we have demonstrated that the pretreatment of our newly designed pH-responsive redox nanoparticle (RNP^N), which tends to accumulate and disintegrate in tumor area, enhances the anti-tumor activity of DOX, because the exposed nitroxide radicals effectively scavenge ROS, which suppress the activation of NF-κB in this area. Our findings also showed that RNP^N protects the cardiac damage by DOX in vivo. It should be noted that LMW-TEMPOL did not show these effects, which was probably due to its non-specific dispersion in entire body. This approach is based on the redox-nanoparticle assisted suppression of oxidative stress in tumor microenvironment, which may open a new paradigm for the design of improved cancer treatments with high chemotherapeutic outcomes, suppressing their adverse effects.

Acknowledgments

We would like to thank Nobuko Nishizawa and Umeko Horiuchi (Graduate School of Pure and Applied Sciences, University of Tsukuba) for their technical assistance. Part of this work was supported by a Grant-in-Aid for Scientific Research A (21240050) and the World Premier

International Research Center Initiative (WPI Initiative) on Materials Nanoarchitronics from the Ministry of Education, Culture, Sports, Science and Technology (MEXT) of Japan.

REFERENCES

[1] A. Mantovani, P. Allavena, A. Sica, F. Balkwill, Cancer-related inflammation, Nature, 454 (2008) 436-444.

[2] M. Jinushi, S. Chiba, H. Yoshiyama, K. Masutomi, I. Kinoshita, H. Dosaka-Akita, H. Yagita, A. Takaoka, H. Tahara, Tumor-associated macrophages regulate tumorigenicity and anticancer drug responses of cancer stem/initiating cells, Proc Natl Acad Sci U S A, 108 (2011) 12425-12430.

[3] I.T. Hwang, Y.M. Chung, J.J. Kim, J.S. Chung, B.S. Kim, H.J. Kim, J.S. Kim, Y.D. Yoo, Drug resistance to 5-FU linked to reactive oxygen species modulator 1, Biochem Biophys Res Commun, 359 (2007) 304-310.

[4] G.Y. Liou, P. Storz, Reactive oxygen species in cancer, Free Radic Res, 44 (2010) 479-496.

[5] M. Bentires-Alj, V. Barbu, M. Fillet, A. Chariot, B. Relic, N. Jacobs, J. Gielen, M.P. Merville, V. Bours, NF-kappaB transcription factor induces drug resistance through MDR1 expression in cancer cells, Oncogene, 22 (2003) 90-97.

[6] B.B. Aggarwal, S. Shishodia, Y. Takada, S. Banerjee, R.A. Newman, C.E. Bueso-Ramos, J.E. Price, Curcumin suppresses the paclitaxel-induced nuclear factor-kappaB pathway in breast cancer cells and inhibits lung metastasis of human breast cancer in nude mice, Clin Cancer Res, 11 (2005) 7490-7498.

[7] S. Oiso, R. Ikeda, K. Nakamura, Y. Takeda, S. Akiyama, H. Kariyazono, Involvement of NF-kappaB activation in the cisplatin resistance of human epidermoid carcinoma KCP-4 cells, Oncol Rep, 28 (2012) 27-32.

[8] S. Granados-Principal, J.L. Quiles, C.L. Ramirez-Tortosa, P. Sanchez-Rovira, M.C. Ramirez-Tortosa, New advances in molecular mechanisms and the prevention of adriamycin toxicity by antioxidant nutrients, Food Chem Toxicol, 48 (2010) 1425-1438.

[9] S.M. DeAtley, M.Y. Aksenov, M.V. Aksenova, B. Jordan, J.M. Carney, D.A. Butterfield, Adriamycin-induced changes of creatine kinase activity in vivo and in cardiomyocyte culture, Toxicology, 134 (1999) 51-62.

[10] H. Wang, M. Li, J.J. Rinehart, R. Zhang, Pretreatment with dexamethasone increases antitumor activity of carboplatin and gemcitabine in mice bearing human cancer xenografts: in vivo activity, pharmacokinetics, and clinical implications for cancer chemotherapy, Clin Cancer Res, 10 (2004) 1633-1644.

[11] H. Wang, M. Li, J.J. Rinehart, R. Zhang, Dexamethasone as a chemoprotectant in cancer chemotherapy: hematoprotective effects and altered pharmacokinetics and tissue distribution of carboplatin and gemcitabine, Cancer Chemother Pharmacol, 53 (2004) 459-467.
[12] H. Wang, Y. Wang, E.R. Rayburn, D.L. Hill, J.J. Rinehart, R. Zhang, Dexamethasone as a chemosensitizer for breast cancer chemotherapy: potentiation of the antitumor activity of adriamycin, modulation of cytokine expression, and pharmacokinetics, Int J Oncol, 30 (2007) 947-953.
[13] S. Kokura, N. Yoshida, N. Sakamoto, T. Ishikawa, T. Takagi, H. Higashihara, N. Nakabe, O. Handa, Y. Naito, T. Yoshikawa, The radical scavenger edaravone enhances the anti-tumor effects of CPT-11 in murine colon cancer by increasing apoptosis via inhibition of NF-kappaB, Cancer Lett, 229 (2005) 223-233.
[14] S. Suy, J.B. Mitchell, A. Samuni, S. Mueller, U. Kasid, Nitroxide tempo, a small molecule, induces apoptosis in prostate carcinoma cells and suppresses tumor growth in athymic mice, Cancer, 103 (2005) 1302-1313.
[15] H. Yoshioka, H. Tanizawa, T. Ogata, S. Kazama, A novel spin probe with long life in vivo for ESR imaging, Biol Pharm Bull, 18 (1995) 1572-1575.
[16] W.J. Welch, M. Mendonca, J. Blau, A. Karber, K. Dennehy, K. Patel, Y.S. Lao, P.A. Jose, C.S. Wilcox, Antihypertensive response to prolonged tempol in the spontaneously hypertensive rat, Kidney Int, 68 (2005) 179-187.
[17] E. Monti, R. Supino, M. Colleoni, B. Costa, R. Ravizza, M.B. Gariboldi, Nitroxide TEMPOL impairs mitochondrial function and induces apoptosis in HL60 cells, J Cell Biochem, 82 (2001) 271-276.
[18] E. Alpert, H. Altman, H. Totary, A. Gruzman, D. Barnea, V. Barash, S. Sasson, 4-Hydroxy tempol-induced impairment of mitochondrial function and augmentation of glucose transport in vascular endothelial and smooth muscle cells, Biochem Pharmacol, 67 (2004) 1985-1995.
[19] T. Yoshitomi, D. Miyamoto, Y. Nagasaki, Design of core--shell-type nanoparticles carrying stable radicals in the core, Biomacromolecules, 10 (2009) 596-601.
[20] T. Yoshitomi, R. Suzuki, T. Mamiya, H. Matsui, A. Hirayama, Y. Nagasaki, pH-sensitive radical-containing-nanoparticle (RNP) for the L-band-EPR imaging of low pH circumstances, Bioconjug Chem, 20 (2009) 1792-1798.
[21] T. Yoshitomi, Y. Nagasaki, Nitroxyl radical-containing nanoparticles for novel nanomedicine against oxidative stress injury, Nanomedicine (Lond), 6 (2011) 509-518.
[22] Y. Nagasaki, Nitroxide radicals and nanoparticles: a partnership for nanomedicine radical delivery, Ther Deliv, 3 (2012) 165-179.

[23] R.A. Gatenby, R.J. Gillies, Why do cancers have high aerobic glycolysis?, Nat Rev Cancer, 4 (2004) 891-899.
[24] P. Chonpathompikunlert, T. Yoshitomi, J. Han, H. Isoda, Y. Nagasaki, The use of nitroxide radical-containing nanoparticles coupled with piperine to protect neuroblastoma SH-SY5Y cells from Abeta-induced oxidative stress, Biomaterials, 32 (2011) 8605-8612.
[25] P. Chonpathompikunlert, T. Yoshitomi, J. Han, K. Toh, H. Isoda, Y. Nagasaki, Chemical nanotherapy: nitroxyl radical-containing nanoparticle protects neuroblastoma SH-SY5Y cells from Abeta-induced oxidative stress, Ther Deliv, 2 (2011) 585-597.
[26] P. Chonpathompikunlert, C.H. Fan, Y. Ozaki, T. Yoshitomi, C.K. Yeh, Y. Nagasaki, Redox nanoparticle treatment protects against neurological deficit in focused ultrasound-induced intracerebral hemorrhage, Nanomedicine (Lond), 7 (2012) 1029-1043.
[27] T. Yoshitomi, A. Hirayama, Y. Nagasaki, The ROS scavenging and renal protective effects of pH-responsive nitroxide radical-containing nanoparticles, Biomaterials, 32 (2011) 8021-8028.
[28] A. Marushima, K. Suzuki, Y. Nagasaki, T. Yoshitomi, K. Toh, H. Tsurushima, A. Hirayama, A. Matsumura, Newly synthesized radical-containing nanoparticles enhance neuroprotection after cerebral ischemia-reperfusion injury, Neurosurgery, 68 (2011) 1418-1425; discussion 1425-1416.
[29] Y. Matsumura, H. Maeda, A new concept for macromolecular therapeutics in cancer chemotherapy: mechanism of tumoritropic accumulation of proteins and the antitumor agent smancs, Cancer Res, 46 (1986) 6387-6392.
[30] B.P. Soule, F. Hyodo, K. Matsumoto, N.L. Simone, J.A. Cook, M.C. Krishna, J.B. Mitchell, The chemistry and biology of nitroxide compounds, Free Radic Biol Med, 42 (2007) 1632-1650.
[31] C.G. Pham, C. Bubici, F. Zazzeroni, S. Papa, J. Jones, K. Alvarez, S. Jayawardena, E. De Smaele, R. Cong, C. Beaumont, F.M. Torti, S.V. Torti, G. Franzoso, Ferritin heavy chain upregulation by NF-kappaB inhibits TNFalpha-induced apoptosis by suppressing reactive oxygen species, Cell, 119 (2004) 529-542.
[32] L.B. Vong, T. Tomita, T. Yoshitomi, H. Matsui, Y. Nagasaki, An orally administered redox nanoparticle that accumulates in the colonic mucosa and reduces colitis in mice, Gastroenterology, 143 (2012) 1027-1036 e1023.
[33] B. Khodr, Z. Khalil, Modulation of inflammation by reactive oxygen species: implications for aging and tissue repair, Free Radic Biol Med, 30 (2001) 1-8.

Figure Legends:

Figure 1. Schematic illustration of (a) pH-sensitive RNP^N, which is a core-shell type of self-assembling polymeric micelle that is 40 nm in diameter and prepared using poly(ethylene glycol)-*b*-poly[4-(2,2,6,6-tetramethylpiperidine-*N*-oxyl)aminomethylstyrene] (PEG-*b*-PMNT) amphiphilic diblock copolymers; and (b) the effective accumulation and disintegration of RNP^N in the tumor area.

Figure 2. **(a,b)** Distribution profiles of RNP^N (white circle) and low-molecular-weight (LMW) 4-hydroxy-2,2,6,6-tetramethylpiperidine-*N*-oxyl (TEMPOL) (block triangle) in (a) blood and (b) tumor tissue from tumor-bearing mice, as determined by electron spin resonance (ESR) measurement. The data are expressed as means ± SEM; n = 5. **(c-f)** The ESR spectra of (c) LMW-TEMPOL in blood, (d) LMW-TEMPOL in tumor, (e) RNP^N in blood, and (f) RNP^N in tumor at 15 min after intravenous administration are shown. All samples were oxidized by potassium ferricyanide ($K_3[Fe(CN)_6]$).

Figure 3. Suppressive effects of RNP^N on the activation of NF-κB. (a) Western blot analysis of NF-κB expression in colon-26 cells treated with RNP^N. (b) The graph represents the densitometry average of three representative blots. Values are expressed as mean ± SEM. **P* < 0.05 compared with controls; Student's *t*-test; n = 3.

Figure 4. Suppressive effect of pretreatment with RNP^N on the generation of superoxide anions and TNF-α in tumors. (a) Amounts of superoxide in tumor tissue were measured using dihydroethidium (DHE). Superoxide values were expressed as the value related to the fluorescent intensity of the saline group. Values are expressed as mean ± SEM. **P* < 0.05 compared with the saline group; ANOVA; n = 5. (b) The concentration of TNF-α in tumor was measured by enzyme-linked immunosorbent assay (ELISA). Values are expressed as mean ± SEM. **P* < 0.05 compared with the saline group; ANOVA; n = 10.

Figure 5. Effect of RNP^N pretreatment on the antitumor activity of doxorubicin (DOX) in BALB/c mice bearing colon-26 tumors. Animals were intravenously pretreated with RNP^N (100 mg/day for 4 days, days -4 to -1). DOX was intravenously administered at a single dose of 10 mg/kg on day 0. Tumor size is expressed as mean ± SEM. ∗*P* < 0.05 compared with DOX alone; Student's *t*-test; n = 5.

Figure 6. (a,b) Effect of treatment with RNP^N or 4-hydroxy-2,2,6,6-tetramethylpiperidine-*N*-oxyl (TEMPOL) on doxorubicin (DOX)-induced cardiotoxicity, as determined by measurement of the activities of (a) creatine phosphokinase (CPK) and (b) lactate dehydrogenase (LDH) in plasma. The bar graphs represent means ± SEM, **P* < 0.05 compared with DOX alone; Student's *t*-test; n = 6. (c) Amounts of superoxide in heart tissue were measured using dihydroethidium (DHE). Superoxide values were expressed as the value related to the fluorescent intensity of the control group. Values are expressed as mean ± SEM. **P* < 0.05 compared with DOX alone; ANOVA; n = 4. (d) Effect of treatment with RNP^N or LMW-TEMPOL on malonyldialdehyde (MDA) activity in the heart tissue of ICR mice after DOX administration. Values are expressed as mean ± SEM. **P* < 0.05 compared with DOX alone; Student's *t*-test; n = 6.